THERMOMECHANICAL STUDY ON MULTIPLE HINGE CONFIGURATIONS EMPLOYED IN MODULAR MICROSATELLITE DESIGN

Tudor ALEXANDRU[1], Cristina PUPĂZĂ[2], Dorel ANANIA, Claudiu BÎȘU[4]

Abstract: The present paper describes an approach for evaluating the thermal and mechanical behavior of a small satellite aluminum frame. The study takes into account two types of hinge configurations: a torsional and a lamellar spring joint. An equivalent heat flux is derived from the scientific literature. The temperature gradients are used as input in a structural analysis for evaluating the displacements and stress that occurs in the assembly joint locations.

Keywords: thermomechanical, small satellite, heat transfer, simulation

1. INTRODUCTION

The Card-Sat represents a new small satellite concept that is characterized by a slim paralelipipedic shape [1]. Multiple units can be encompassed to form bigger artifacts, like 2U, 3U or 4U. The main purpose of this new concept is to confer small private players an easier and more sustainable access to space [2]. In this regard, the costs associated to the development, launching, and operation are kept to the lowest possible figures. Typical applications include low budget space missions that have educational, earth remote sensing, science or defense purposes. The primary structure of the Card-Sat concept is made of thin aluminum frames. Their design enables the integration of Commercial Off-The-Shelf (COTS) components. Thus, power,

[1] *Lecturer PhD Eng., Robots and Production System Department, University POLITEHNICA of Bucharest, Romania, e-mail: alexandru_tudor_imst@yahoo.com*
[2] *Professor PhD Eng., Robots and Production System Department, University POLITEHNICA of Bucharest, Romania, e-mail: cristinapupaza@yahoo.co.uk*
[3] *Assoc. Professor PhD Eng., Robots and Production System Department, University POLITEHNICA of Bucharest, Romania, e-mail: dorel.anania@upb.ro*
[4] *Assoc. Professor PhD Eng., Robots and Production System Department, University POLITEHNICA of Bucharest, Romania, e-mail: cfbisu@gmail.com*

propulsion or data acquisition subsystems can be included based on the requirements of the stakeholders. The modular design of this small satellite family demands a customizable hinge system that can ensure the self-opening of the frames during the Low Earth Orbit (LEO) deployment process. From this perspective, spring operated joints represent the most attractive solution. The guidelines for sizing such hinge systems are widely available throughout the literature [3-5]. However, the transient heat transfer that occurs in the LEO due to conduction and radiation brings into discussion the risks of mechanical creep [6]. From this perspective, the adequate evaluation of thermal stress and displacement in the mounting locations of the hinges is mandatory [7]. The present paper describes a methodology for simulating a critical temperature profile of a typical CubeSat mission by employing SolidWorks Simulation Transient thermal analysis and the Python Control Systems Library. In the first stage, a black-box modeling approach is completed for evaluating the equivalent heat flux that occurs at primary structure levels. Characteristic curves are depicted from the specialty literature. The step response of the aluminum frame is evaluated under unitary heat flux. This objective is completed in the simulation environment. The resulting first-order system is expressed as a single pole transfer function. By inverting G(s), the output heat flux can be evaluated from the input temperature curve. In the next stage, a thermomechanical analysis is carried out for identifying the equivalent stress and the thermal displacements that occur at the level of the aluminum frame, in the mounting location of the hinges. Two different configurations are taken into account: torsional and lamellar spring joints. The results achieved are further used in the manufacturing stage for deciding the optimal geometric dimensioning and tolerancing.

2. THEORETICAL CONSIDERATIONS

Heat transfer in the LEO occurs mainly due to conduction and radiation, convection being negligible [8]. From this perspective, an array of thermal resistors can be employed to describe the main junctions that occur between the components of a single unit CardSat assembly (Fig.1).

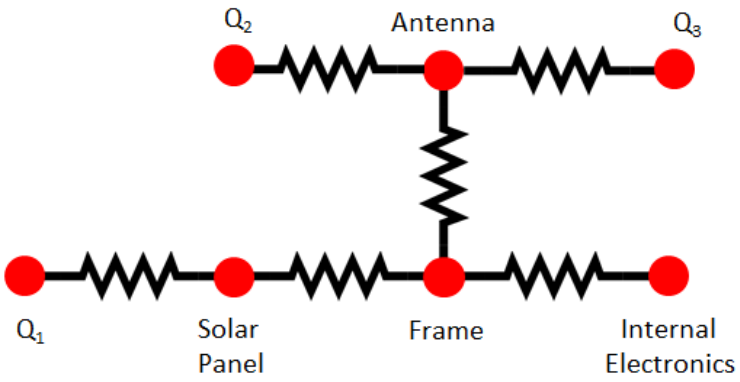

Fig.1. The equivalent thermal network for a single unit CardSat

In Figure 1, Q_1 to Q_3 represent the heat fluxes that are caused by the direct solar flux, albedo and the Earth infrared radiation. The resulting energy is transferred to the secondary structure elements, such as the solar panels and the antennas. A temperature gradient occurs at the level of the frame which represents either the hot surface (during eclipse) or the cold surface (when the heat generating nodes are exposed to irradiance). On the other hand, the internal electronics transfers heat to the frame by mutual body radiation and / or conduction.

A spacecraft that is orbiting in the LEO is subjected to electromagnetic radiation from three distinct sources:

1. **The solar flux** represents the most dominant heat source in the LEO. The amount of energy that is absorbed by a surface (in W) can be estimated by using [9]:

$$\dot{q}_{solar} = \alpha \cdot A \cdot S \cdot \cos\theta \tag{1}$$

Where: α represents the absorptivity of the surface, A the surface area, S the solar constant and θ the incident angle. The solar constant is defined as the radiation that falls on a surface that is normal to the line from the Sun, per unit time outside the atmosphere, at one astronomical unit. The solar constant has a value of 1371 W/m^2, with an uncertainty of about 10 W/m^2 [10].

2. **The albedo radiation** represents the solar energy that is reflected by the Earth. This heat source is only applicable when a portion of the Earth that is seen by the satellite is sunlight [11].Typical albedo factors vary between 0.25 and 0.55, depending on the characteristic of the surface (in terms of color and roughness). The incident albedo radiation can be calculated as [9]:

$$\dot{q}_{albedo} = \frac{\dot{q}_{solar}}{\cos\theta} \cdot A_f \cdot F_{Earth \to Surface} \tag{2}$$

Where: A_f represents the albedo factor and $F_{Earth \to Surface}$ the view factor (or the fraction of energy that is exhibited by the Earth and absorbed by the external surface of the spacecraft. Definition of view factors can be depicted in [12].

3. **The Earth infrared** represents the amount of energy that is emitted by the Earth as long-wave infrared radiation that has a black body spectrum with a characteristic average temperature of 288 K [11]. The amount of infrared radiation that is absorbed by an external surface of a LEO spacecraft can be expressed as:

$$\dot{q}_{IR} = \sigma \cdot \varepsilon \cdot A \cdot F_{Earth \to Surface} T_E^{\ 4} \tag{3}$$

Where: σ represents the Stefan-Boltzmann constant, ε the surface emissivity and T_E the ideal radiator or black body Earth temperature. The average value of the Earth emitted infrared radiation is 230 W m^2 [13].

3. THE STUDIED ASSEMBLY

The studied assemblies comprise two panels which are held together by lamellar or torsional spring joints. Figure 2 –a and b depicts the two configuration.

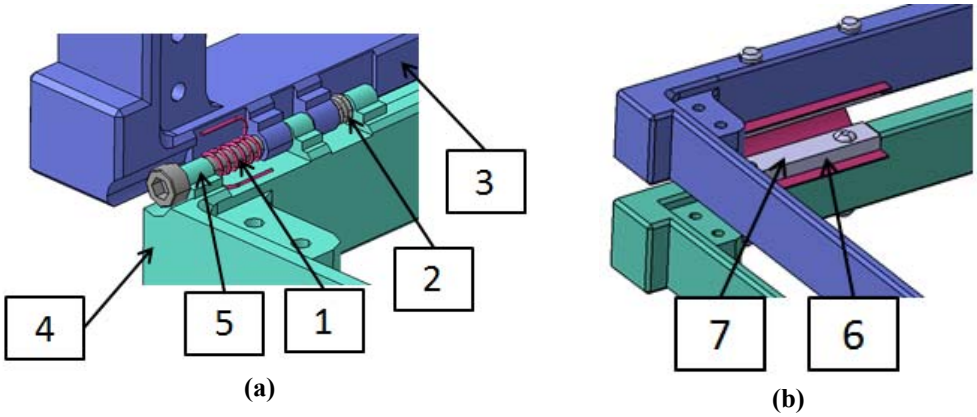

Fig. 2. Information regarding the studied assembly

A description of them is presented bellow:

- **Torsional spring joint:** the hinge system comprises two springs (1 and 2). The first one represents a torsional spring that ensures a moment reaction when the two frames (3, 4) are released from their holding position. The second spring is employed as a solution for thermal displacement feedback, when one of the knuckles (5) suffers creep.
- **Lamellar spring joint:** the hinge system comprises a single lamellar spring (6) that is attached to the two panels by means of two spacers (7). When the two frames are released, the pre-stressed spring generates the bending moment required for opening the frames in their operational position.

During the analysis, only one frame is taken into account. Information regarding the material properties is depicted in Table 1 [14].

Table 1. **Material properties for the studied frames**

Material Name	Thermal properties			Mechanical properties		
	Thermal conductivity	Density	Specific Heat	Modulus of Elasticity	Poisson Ratio	Coefficient of Thermal Expansion
AL 6068 Alloy	179 W/m-K	2.71 g/cm^3	0.886 J/g°C	84.1 GPa	0.327	23.0 µm/m°C

4. THE PROPOSED METHODOLOGY

A schematic representation of the proposed methodology is depitected in Figure 3.

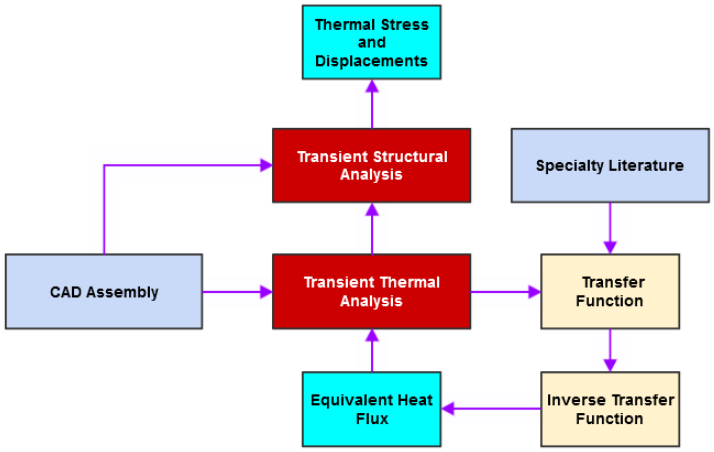

Fig.3. Schmeatic representation of the proposed methodology

In the first stage, the CAD Assembly (including the aluminum frame and the joint systems) is imported to the simulation environment. Topological operations are carried out to simplfy the model prior to the mesh generation stage. Two types of simulations are carried out:

1. **Transient Thermal Analysis:** the objective of this analysis is to capture the time vs. temperature gradients of the assembly. Given the fact that only a fraction of the total irradience energy is absorbed by the frames, an equivalent heat flux is requiered for achieving realistic results. In this regard, temperature curves from the literature are employed. The strucutre is simulated by applying a unit heat flux on the front surfaces. This approach facilitates the estimation of a first order system that describes the dynamic relationship between the input heat flux and output temperature increase. By inverting the resulting first order system, the energy requiered to increase the temperature of the frame to a given value is identified.

2. **Transient Structural Analysis:** the objective of this analysis is to identify the thermal stress and displacement, by considering the temperature gradients from the thermal analysis as input. The results are processed in the assembly joint locations.

5. TRANSIENT THERMAL ANALYSIS

The transient thermal analysis is carried out by considering the hottest orbit in which the microsatellite will operate (with an inclination angle θ of 90°). A unitary heat flux that is applied on the front surface of the aluminum frames to evaluate their response under step-loading.

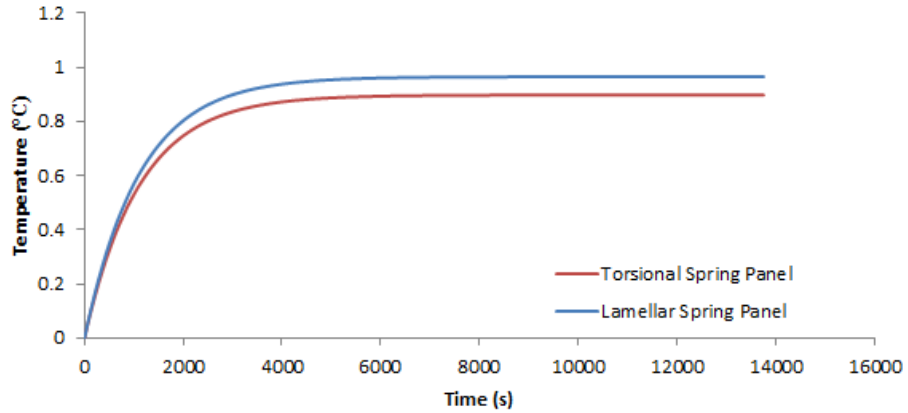

Fig.4. Step-response of the two frame types under unitary heat flux

A single pole transfer function can be derrived from both curves, given their first-order system behavior. This objective is achieved by evaluating the time constant and temperature gain of the two configuarions (Table 2).

Table 2. **Temperature gain and time constants of the temperature curves**

Configuration	Temperature gain	Time constant
Torsional Spring Panel	0.89	3420
Lamellar Spring Panel	0.96	4321.5

In the next stage, the total heat flux that acts on the aluminum frames is derrived from a typical CubeSat mission [15]. At first, the temperaturess measured on the primary structure for various inclination angles are analyzed. The most critical mission segment for the worst hot case occurs on panel 5. The structure is subjected to the direct solar heat flux along the entire orbit reaching temperatures of 77°C (Fig.5).

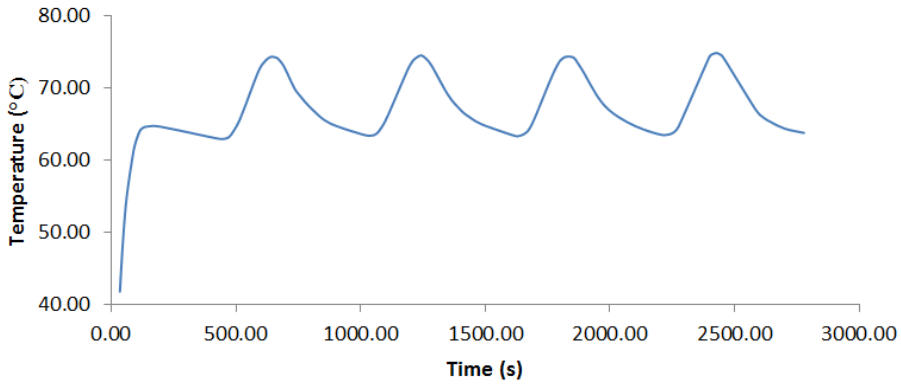

Fig.5. Critical hot orbit temperatures occuring on the primary structure of CubeSat – Panel 5

Based on Figure 5, the equivalent heat flux that can be applied to the frame is identified by inverting the transfer functions from table 2. Thus, the temperature profile from Figure 5 is used as input and the output of the first order systems corresponds with the heat dissipation (Fig.6).

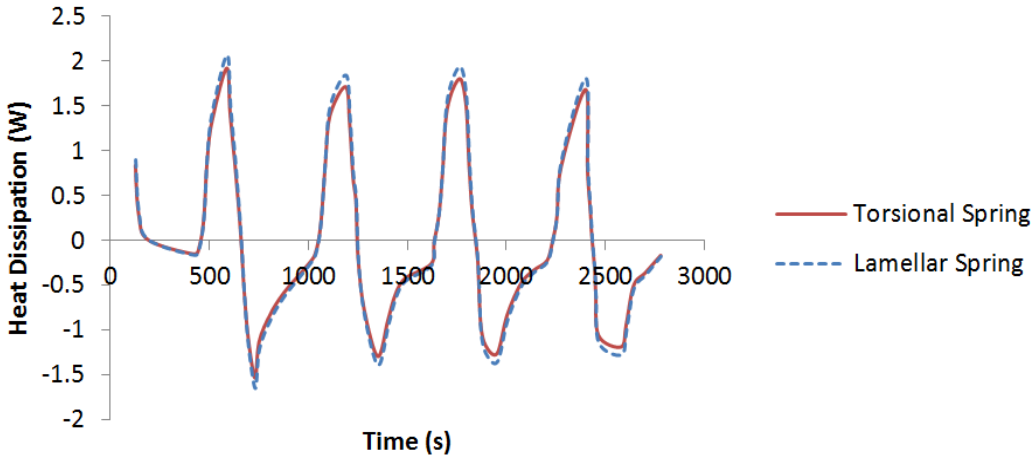

Fig.6. Equivalent heat dissipation achieved by inverting G(S)

6. TRANSIENT STRUCTURAL ANALYSIS

The temperature gradients from the thermal analysis are used for identifying the thermal displacements and stress that occurs in the in the assembly joint locations.

Figure 7 depicts the radial displacements of the studied configurations.

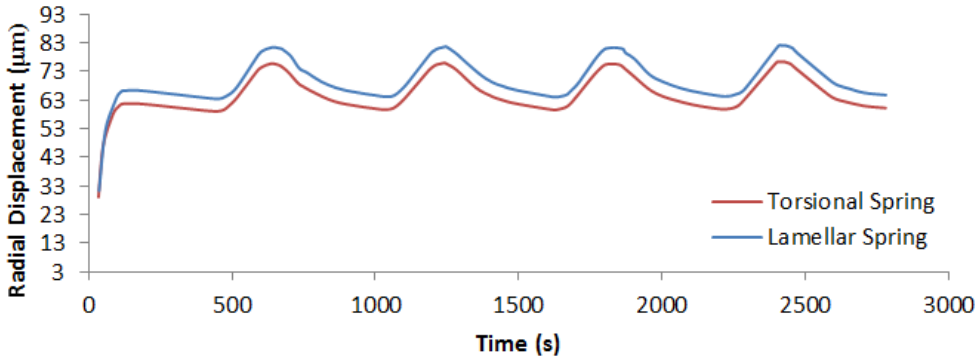

Fig.7. Radial displacements of the frames in the assembly joint locations

The maximum radial displacements have values of 82µm in case of the torsional spring configuration and 76 µm in case of the lamellar spring configuration. Both values occur after 644 seconds simulation time, in accordance with the applied heat flux. Afterwards, the slope of the two curves follows a cyclic tendency.

Figure 8 depicts the axial displacements of the studied configurations.

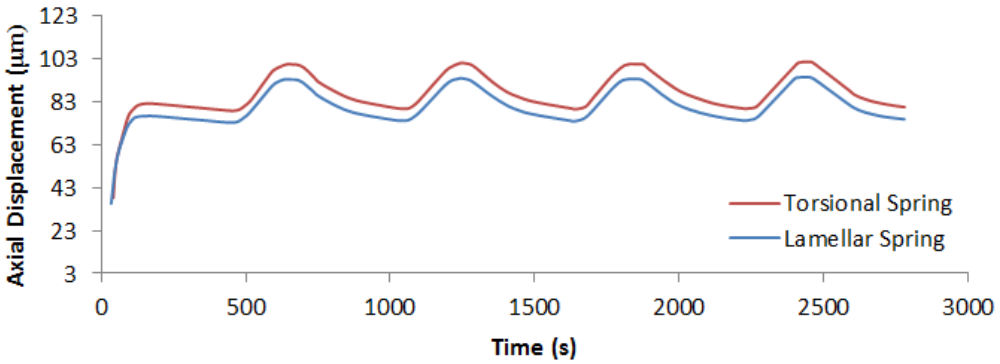

Fig.8. Axial displacements of the frames in the hinge assembly locations

In this case, the torsional spring configuration achieves greater values (101 µm) than compared to the lamellar spring configuration (94.2 µm). Similar to the previous case, the critical results occur after 644 seconds simulation time.

The structural integrity of the frame can only be confirmed by evaluating the stress occuring on the entire structure. By knowing that the Yield strength of the AL 6068 Alloy is 150 MPa, a safety factor can be determined based on the maximum calculated values. Figure 9 depicts the Equivalent Von Mises Stress for both studied configurations.

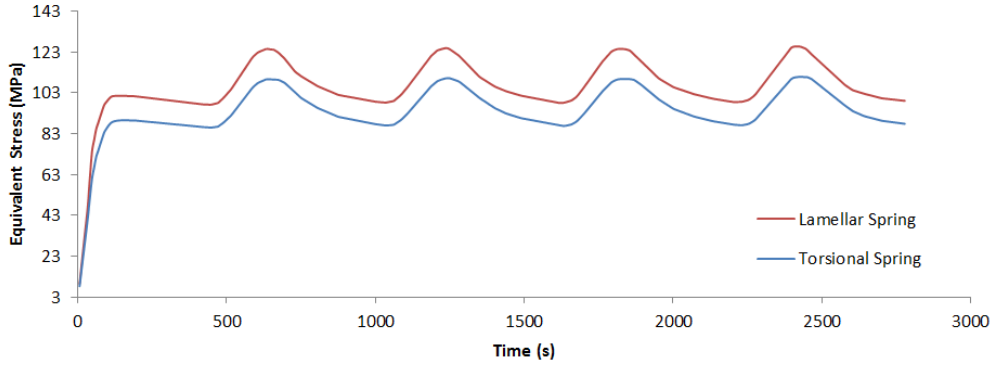

Fig.9. Equivalent Von Mises Stress for both studied configurations

The maximum value of 125.6 MPa occurs in case of the lamellar spring configuration, while the torsional spring configuration achieves 110.8 MPa. In both cases, the safety factors are >1. However, due to the cyclic nature of the applied load, thermal fatigue can be the most likely cause of structural failure.

7. CONCLUSIONS

In the present research, the thermomechanical analysis of two different aluminum frame configurations is carried out by considering a severe thermal cycle. The equivalent heat flux that acts on the front surfaces of the model is derived from the scientific literature. This objective is completed by employing an inverted transfer function approach. The results achieved from the thermal analysis are further used in the transient structural simulation environment. Thus, the effects of structural dilatation and contraction can be captured. The maximum radial and axial displacements are then employed for deciding the optimal geometric dimensioning and tolerancing. On the other hand, the calculated Equivalent stress offers an insight regarding the structural integrity. Due to the fact that the safety factors have values are lower than 1.5, it is expected that thermal fatigue failure can occur. Furthermore, the cyclic behavior of the applied heat flux enhances this effect even more. From this perspective, a parametric study is required for adjusting the chamfers of the geometric model.

AKNOWLEDGEMENTS

This work was supported by the 1st priority axis of "The Competitiveness Operational Program" [ID / Cod MySMIS: 120353] in the framework of "Advanced Technologies for Manufacturing and Testing of Advanced Materials in the Aerospace Domain", Contract number [402/390078/24.12.2021].

REFERENCES

[1]. **Totu, A.,** *Small-size artificial satellite - "card-sat"*, United States Patent Application Publication: US 2020/0391886 A1, 2020.
[2]. **MAZAROM IMPEX SRL**, *CARD-SAT Solution*. Retrieved November 30, 2022, from https://www.card-sat.com/index.php/en/.
[3]. **Murphy, T., Kanaber, J., Koehler, C,.** *PEZ: expanding CubeSat capabilities through innovative mechanism design*, 25th Annual AIAA/USU Conference on Small Satellites, 2011, pp. 1-4.
[4]. **Langer, M., Olthoff, C., Datshvili, L., Baier, H., Maghaldadze, N., Walter, U.,** *Deployable structures in the CubeSat program MOVE*, Proceedings of the 2nd International Conference Advanced Lightweight Structures and Reflector Antennas, 2014, pp. 224-233.
[5]. **Ziade, E., Patmont, C. S., Fritz, T. A.,** *Design and characterization of a spring steel hinge for deployable CubeSat structures*, Journal of Small Satellites, 5(1), 2016, pp. 407-418.
[6]. **Kobelev, V.,** *Durability of springs*, Springer International Publishing, Wien, 2018.
[7]. **Muhammed, L. N., Ugheoke, B. I., Nwachukwu, D. O.,** *Modeling and simulation of the kinematic behavior of the deployment mechanism of solar array for a 1-U CubeSat*, Engineering Reports, 2022, pp.1-26.
[8]. **Miao, J., Zhong, Q., Zhao, Q., Zhao, X.,** *Spacecraft thermal control technologies*. Singapore: Springer, 2021.

[9]. **Foster, I.,** *Small Satellite Thermal Modeling Guide*, Air Force Research Laboratory, 2022.
[10]. **Rickman, S.L.,** *Introduction to On-Orbit Thermal Environments*, in Thermal and Fluids Analysis workshop, Cleveland, 2014.
[11]. **Boushon, K.E.,** *Thermal Analysis and Control of Small Satellites in Low Earth Orbit*, Missouri University of Science and Technology, 2018.
[12]. **Howell, D.J.,** *A Catalog of Radiation Heat Transfer*, Retrieved November 30, 2022, from http://www.thermalradiation.net/tablecon.html#C1.
[13]. **Gilmore, D.J.,** *Spacecraft Thermal Control Handbook*, Volume 1: Fundamental Technologies, El Segundo Boulevard: The Aerospace Press, 2002.
[14]. **MATWEB LLC.,** *AL6068 Properties*, Retrieved November 30, 2022, from https://www.matweb.com/.
[15]. **Piedra, S., Torres, M., Ledesma, S.,** *Thermal numerical analysis of the primary composite structure of a CubeSat*, Aerospace, 6(9), 2019, pp. 97-111.
[16]. **Popescu, F.D., Radu, S.M., Andraş, A., Brînaş, I., Budilică, D.I., Popescu, V.,** *Comparative Analysis of Mine Shaft Hoisting Systems' Brake Temperature Using Finite Element Analysis (FEA)*, Materials, 2022, 15, 3363.